General Disclaimer

One or more of the Following Statements may affect this Document

- This document has been reproduced from the best copy furnished by the organizational source. It is being released in the interest of making available as much information as possible.

- This document may contain data, which exceeds the sheet parameters. It was furnished in this condition by the organizational source and is the best copy available.

- This document may contain tone-on-tone or color graphs, charts and/or pictures, which have been reproduced in black and white.

- This document is paginated as submitted by the original source.

- Portions of this document are not fully legible due to the historical nature of some of the material. However, it is the best reproduction available from the original submission.
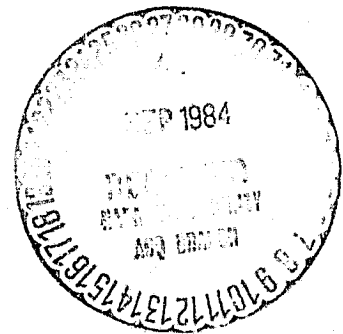
SEVENTH QUARTERLY REPORT
ON

"SPECTRORADIOMETRIC CALIBRATION OF THE
THEMATIC MAPPER AND MULTISPECTRAL SCANNER SYSTEM"

Contract Number NAS5-27382
For the Period: 1 May 1984 - 1 August 1984

NASA/Goddard Space Flight Center
Greenbelt MD 20771

James M. Palmer, Co-Investigator
Philip N. Slater, Principal Investigator

Optical Sciences Center
University of Arizona
Tucson, Arizona 85721

INTRODUCTION

This is the seventh quarterly report on Contract NAS5-27382 entitled, "Spectroradiometric Calibration of the Thematic Mapper and the Multispectral Scanner System." In this report, we summarize the reduction of the data measured on July 8, 1984 at White Sands, New Mexico. The radiances incident at the entrance pupil of the Landsat 5 sensors have been computed for bands 1-4. When these are compared to the digital counts of the TM image, we will have the ground based calibration of this sensor. The image has been received from Goddard SFC and is presently being analyzed.

JULY 8, 1984 CALIBRATION

Field Measurements

This was our first opportunity to acquire on-site measurements at White Sands in conjuction with Thematic Mapper imagery from Landsat 5. Imagery was not available for previous trips due to cloud cover. Assisting in the field measurements were Harumi Aoki, Ken Castle, Barbara Capron, Madgeleine Dinguirard, Ron Holm, Ray Jackson, Carol Kastner, Amy Phillips, Rich Savage, and Phil Slater. The instrumentation on hand included two Barnes radiometers, the cart and yoke, an old model of Reagan's radiometer, both of the Castle spectropolarimeters, four polycorders, a printer, the Compaq computer, and two 2 X 2 ft standard reflectance panels.

Sunrise on the morning of July 8th was at 6:10 a.m. New Mexico was on Mountain Daylight Time (MDT) this time of year, as are the times quoted here. The Reagan instrument was set up and began acquiring solar irradiance measurements at 7:15 a.m. (airmass 4). Rich Savage took temperature, humidity, and pressure readings there at Chuck site. He also arranged for a nearby radiosonde ascent. These data are presented in Appendix B.

Two test sites had been laid out on the previous trip. Each was a 4 X 4 pixel grid, aligned with the east/west scan lines expected of Landsat. A road with a 120° bend separated the two sites, and will facilitate the identification of the sites on the digital TM imagery. Each site was measured with a Barnes radiometer. Starting at the center of

each 30 X 30 meter pixel, five reflectance measurements were taken of the gypsum sands, within an area of about 5. X 0.5 meters. Reflectance panel readings were taken periodically during the course of these measurements. (Both the $BaSO_4$ and Halon panels were recalibrated by Che Nianzeng immediately upon our return.) The data were averaged and recorded on polycorders. The site to the North of the road was scanned using the Purdue radiometer (one of the Barnes), mounted on the cart with the $BaSO_4$ panel. Data were taken from 11 to 11:20 a.m. The south site was scanned simultaneously with an USDA Barnes attached to a yoke. A Halon panel was used as the reference here. In addition to the two 4 X 4 pixel areas, two small areas were scanned near the van. This was done between 10:20 and 11:40 a.m. These areas were selected for their contrast, representing extremes of light and dark for the local area. They will later be used in conjunction with aerial photography to map the reflectance of the entire area. Finally, diffuse to direct measurements were taken between 8:30 and 10:20 a.m. These were made by comparing the radiance reflected from the ground to that radiance measured when the sun was blocked with a styrofoam parasol. These data can be used for comparison with the radiative transfer code, to verify our atmospheric models.

A helicopter overflight was arranged for this trip. Jack Rees and co-pilot Keys piloted the helicopter and Jason Penny, PFC, was the photographer. The flight was almost exactly one full hour. It had the dual purpose of recording radiance at intermediate altitudes, again for comparison to the radiative transfer code output, and photographing the sites. Several slides have been scanned, using a microdensitometer, and will be used to characterize the ground reflectance. Five rolls of

Ektachrome, ASA 100, were shot. All photos were taken at 1/500th of a second, with a 200 mm focal length lens. A series were taken at 6,000, 2,000, and 500 ft., AGL (above ground level). The photos were bracketed from F/16 to F/22, in half F/stop increments. Those taken at 2,000 ft. were particulary suited to our needs. Eight colored ground cloths had been laid out to define the two 4 X 4 pixel areas that were measured with the Barnes. We noted that the blue and orange ground cloths were the most visible from the air, as well as being the easiest to see on the color slides.

The field tests of the newly constructed spectropolarimeters will have to wait for our next trip to White Sands. The helicopter instrument suffered from a power failure, and data from the ground instrument, used for solar irradiance measurements, were lost during the TRS-80 to Compaq transfer. Back-up equipment was, however, available that enabled us to conduct an approximate calibration described in the following.

Langley Plot Computations

The Reagan radiometer was cycled through its narrowband filter set 95 times during the course of the morning. Each data set included, to the nearest second, a start and finish time and a voltage reading for each of the 9 spectral filters. These data were used as input to a program which computed solar zenith angle from ephemermis data. Using a refraction correction, airmasses were then calculated for each measurement. Finally, a weighted least squares analysis was used to compute the slope of the natural log voltages versus airmass, at each wavelength. The computed slopes are equivalent to the spectral optical depths of the atmosphere, τ_{ext}, at the time of overpass. Temporal

stability of the atmosphere is assumed. These results are given in Table 1. Also shown are the optical depth components τ_{Mie}, τ_{Ray}, and τ_{oz}. The computation of these components is discussed next.

Using measured atmospheric pressure (883 mbar), τ_{Ray} can be easily computed. After subtracting this from τ_{ext}, a curve is plotted, as in Figure 1a, which contains only Mie and ozone components. To determine τ_{Mie} a curve is fit through all the $\tau_{ext}-\tau_{Ray}$ data points that do not include absorption. Normally this is done by submitting the optical depth values to a routine which fits the data to an equation of the form log $\tau_{Mie}=a_0+a_1\log \lambda+ a_2(\log \lambda)^2$. As many of the spectral filter data sets were rejected, an alternate approach was taken here. These problems arose because the older of the two Reagan radiometers was used. On this instrument the heater was not functioning. The data are less reliable without the temperature stabilization, due to fluctuations in detector responsitivity. This problem is thought to have affected mainly the 0.872 and 1.03 µm channels.

Instead of our normal procedures, therefore, a manual fitting of the data was performed. A curve of the form log $\tau_{Mie}=a_0+a_1\log \lambda$ was assumed (a straight line on this log-log plot). This is an approximation, valid only if the aerosols can be correctly modeled as obeying a Junge radial size distribution, $dn/dr=c\ r^{-(\nu+1)}$. In such a case the data would fall exactly on a line whose slope, a_1, yields the Junge parameter ν via the relationship $a_1=-\nu+2$. By using only the 0.440 and 0.780 µm data points, a slope was determined. At these wavelengths the ozone absorption coefficients are small. Actually, the 0.440 and 0.872 µm pair is prefered, as the absorption coefficients are approximately equal. The

Table 1. Langley Plot Results.

Data from Reagan Radiometer
8 July, 1984
Chuck Site, White Sands, New Mexico

Latitude	32.935°
Longtitude	106.407°
Right Ascension	7.226228 hours
Declination	22.365361°
Difference (Dec)	-419.3 arc-sec
Earth-Sun Distance	1.016701 AU
Pressure	883. mbar

WAV(μm)	τ_{ext}	τ_{Mie}	τ_{Ray}	τ_{oz}
0.4000	0.4426	0.0981	0.3172	0.0000
0.4400	0.3060	0.0922	0.2138	0.0006
0.5217	0.1921	0.0824	0.1063	0.0127
0.6120	0.1543	0.0743	0.0555	0.0246
0.6708	0.1091	0.0699	0.0382	0.0098
0.7120	0.1063	0.0673	0.0300	0.0046
0.7797	0.0842	0.0634	0.0208	0.0027
0.8717	0.0948	0.0589	0.0133	0.0006
1.0303	0.1103	0.0528	0.0068	0.0000

$\log \tau_{Mie} = a_0 + a_1 \log \lambda$; λ in μm
$a_0 = -1.269 \qquad a_1 = -0.654$

$$\tau_{Ray} = \frac{29123.7 \ (n^2-1)^2}{\lambda^4}$$

$$n = 6432.8 + \frac{2949810}{146-\lambda^2} + \frac{25540}{41-\lambda^4}$$

λ in micrometers

$\tau_{oz,\lambda} = NOZ * \alpha_\lambda$
NOZ = columnar ozone

$$= \frac{\tau_{oz,0.612 \ \mu m}}{\alpha_{0.612 \ \mu m}} = 213.2 \ matm-cm$$

α = spectral absorption coefficient

Table 2. Spectral components for TM midband wavelengths.

WAV (μm)	τ_{ext}	τ_{Mie}	τ_{Ray}	τ_{oz}	E_0(mW/cm^2)
0.486	0.2339	0.0864	0.1421	0.0055	175.955
0.571	0.1745	0.0777	0.0735	0.0232	180.580
0.661	0.1226	0.0706	0.0406	0.0114	153.916
0.838	0.0773	0.0605	0.0156	0.0013	104.708

July 8, 1984
Chuck Site

$\bullet\ \tau_{ext}$

$\log \tau_{Mie} = a_0 + a_1 \log \lambda$

$a_0 = -1.26865$

$a_1 = -.6540286$

PRES= 26.08 (in)

NOZ= 213.1507 (matm-cm)

τ_{ext}

$\tau_{Mie} + \tau_{Ray}$

τ_{Ray}

ORIGINAL
OF POOR QUALITY

WAVELENGTH (μm)

(b)

τ

July 8, 1984
Chuck Site

$\bullet\ \tau_{ext}$

$\circ\ \tau_{ext} - \tau_{Ray}$

— τ_{Mie}

$\log \tau_{Mie} = a_0 + a_1 \log \lambda$

$a_0 = -1.26865$

$a_1 = -.6540286$

PRES= 26.08 (in)

NOZ= 213.1507 (matm-cm)

WAVELENGTH (μm)

(a)

τ
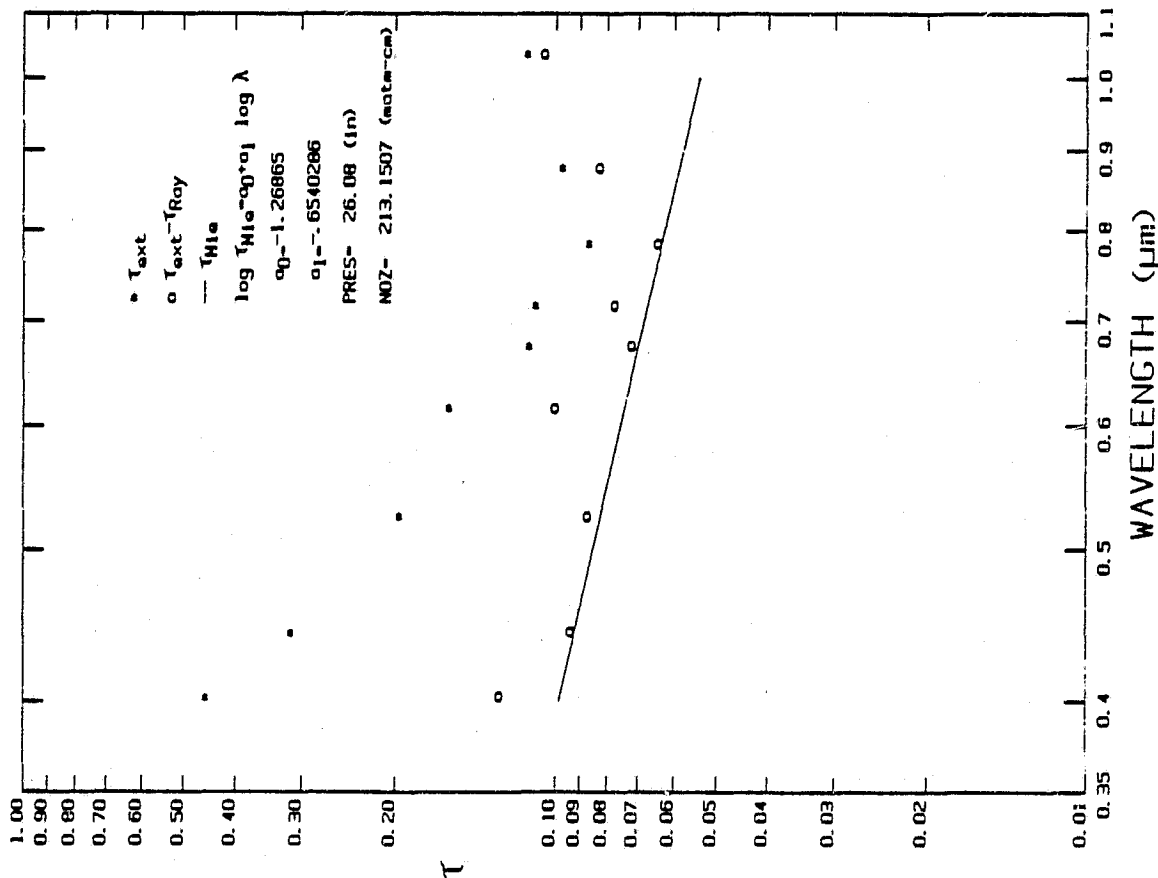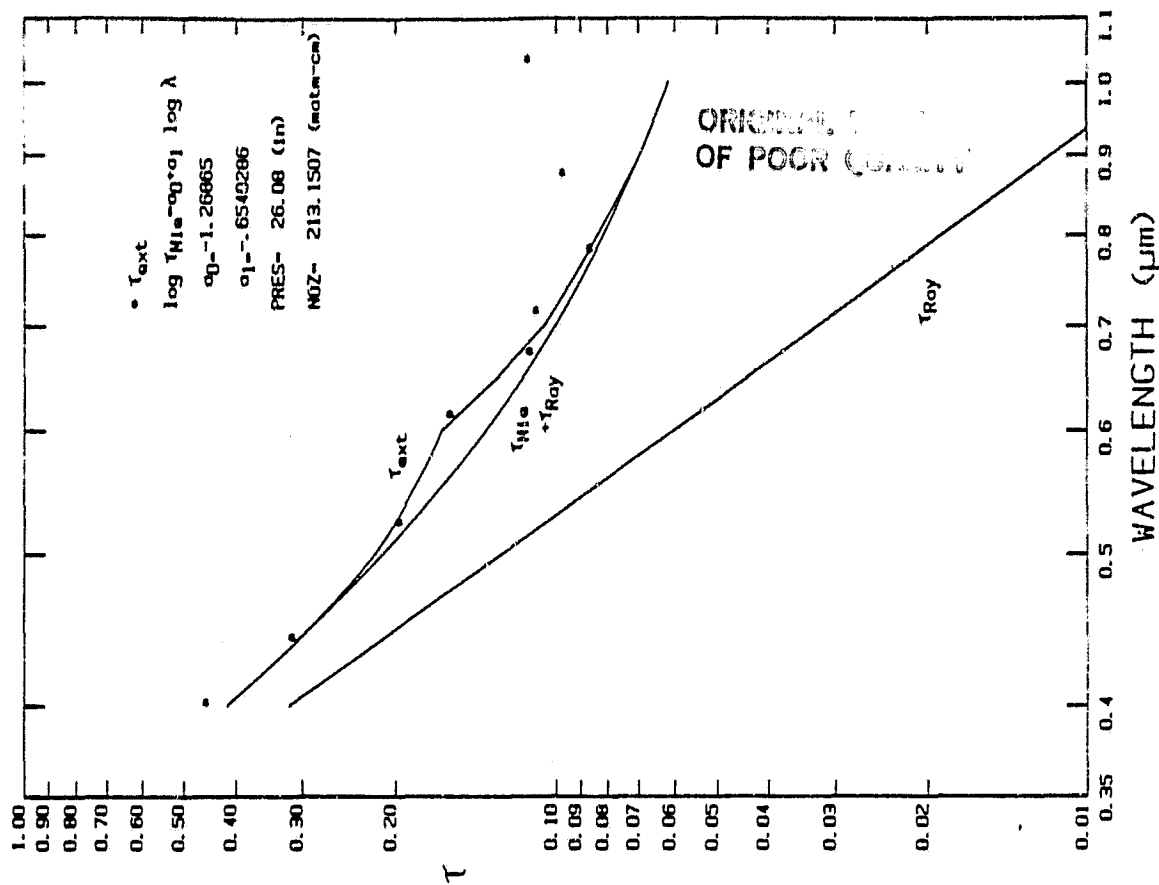
Figure 1. Optical depth versus wavelength data from the Reagan radiometer.

-8-

data at 0.872 μm for this date, however, is unreliable, due to the temperature problem mentioned above. With the given constraints, the slope was found to be $a_1 = -0.654$, thus $\nu = 2.65$, and $a_0 = -1.269$. With these constants the τ_{Mie}, τ_{Ray}, and τ_{oz} components can be computed for any wavelength. Figure 1b shows how each of these components contributes to the total optical depth. Table 2 gives the respective components for the TM midband wavelengths. These data will be used as input to the radiative transfer code. To be complete, a component of τ_{H2O} should be included for band 4. The contribution due to water vapor has not as yet been assessed. Also reported is the exo-atmospheric solar irradiance, as determined from interpolating the data of Neckel and Labs (1981). The midband wavelengths of the TM sensor was computed by Palmer (1984) using the moments method and the pre-flight filter transmittance data.

Panel Calibration

The Herman radiative transfer code requires that the absolute reflectance of the gypsum sands be known. We have instead chosen to use the reflectance factor $R(\theta_z/0°)$. (A discussion of reflectance nomenclature and definitions is given in Appendix A.) Here θ_z is the angle incident upon the gyspum, and $0°$ is the reflected angle, equal to the Thematic Mapper nadir-look angle. By using this quantity, the amount of light reflected in the direction of the TM is accurately characterized. A full BRDF characterization would be prefered. The gain in accuracy is not warranted, however, as the BRDF data would be difficult and time consuming to obtain.

In the field the reflectance factor is measured with one of two Barnes radiometers. As these are uncalibrated they must be used in

conjunction with a reference panel. The reflectance factor of the sands is determined via the relationship

$$R_{sand} = \frac{V_{sand} * R_{ref}}{V_{ref}} . \hspace{2cm} (1)$$

Here V_{sand} and V_{ref} are the output voltages of the Barnes when looking over the sands and reference panel, respectively. These voltages are proportional to the radiance scattered upward and within the instrument's $15°$ field of view (FOV). R_{ref} is the reflectance factor of the panel, as determined in the laboratory. On July 8th one of the radiometers was assigned the Halon panel; the other radiometer was assigned the $BaSO_4$ panel. While looking at the sands, each Barnes was periodically swung over the reference panel and voltage readings were recorded. Upon our return Che Nianzeng calibrated both panels.

The calibration of the panels was conducted at the Optical Sciences Center, in a manner illustrated in Figure 2. A tungsten lamp was put at the focal point of an off-axis parabolic mirror. The emerging planar wavefront thereafter illuminated the reference panel at a known angle. The radiance reflected in a direction normal to the surface was then measured using a radiometer built by Che. Thereafter the reference panel was removed, and a primary standard surface put in its place. This primary standard was a Halon panel which had been calibrated by NBS on February 8, 1984. (They determined the reflectance factor $R_{NBS}(45°/0°)$ for this surface.)

In the first phase of the field panel calibration, the reflectance factor $R_{ref}(45°/0°)$ was determined. This was computed from the following
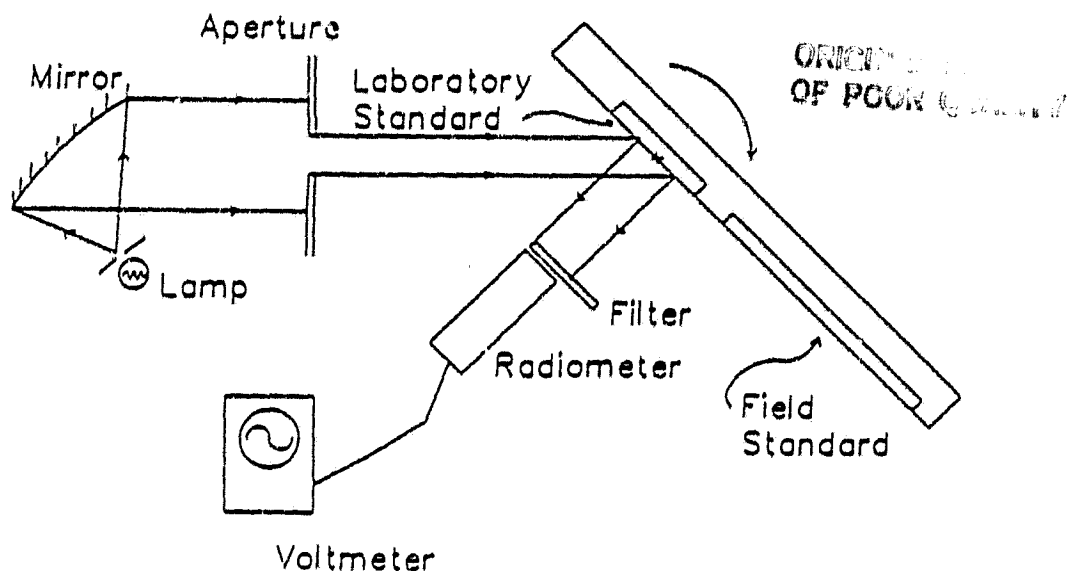
Figure 2. Laboratory set-up for the calibration of field reflectance
           panels.
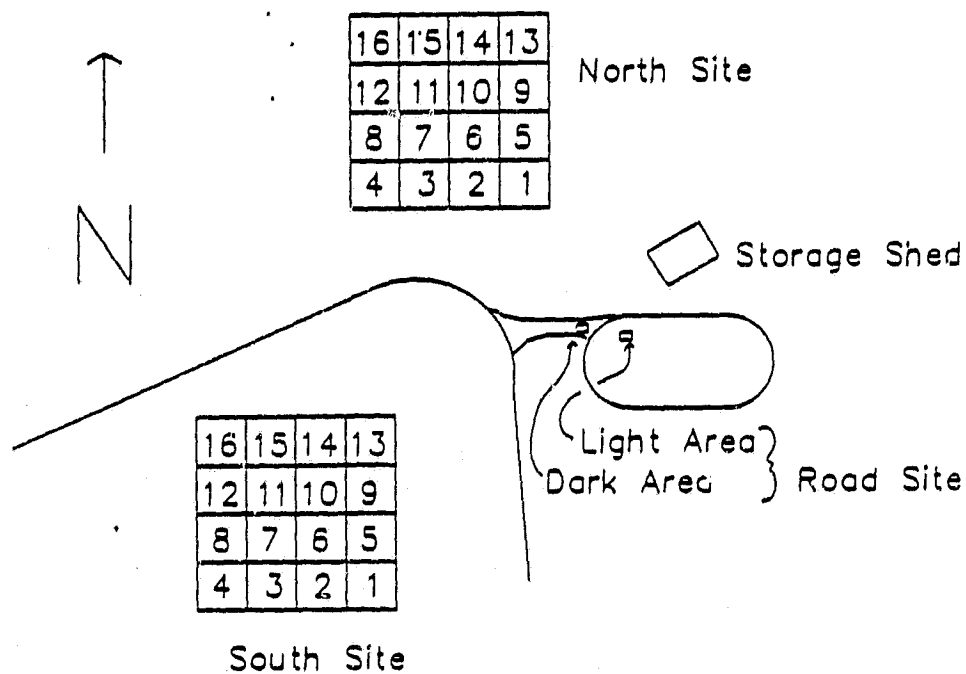
Figure 3. Schematic of Chuck Site test area.

Table 3. Laboratory calibration of $BaSO_4$ panel.

THE REFLECTANCE FACTOR OF $BaSO_4$ PANEL NO.5

Irradiance Angle(deg.)	430-470nm	530-570nm	630-670nm	830-870nm
10	1.0420	1.0355	1.0205	0.9858
15	1.0196	1.0138	0.9990	0.9651
20	1.0011	0.9945	0.9807	0.9479
25	0.9836	0.9779	0.9642	0.9331
30	0.9668	0.9610	0.9479	0.9185
35	0.9499	0.9449	0.9327	0.9045
40	0.9326	0.9279	0.9169	0.8905
45	0.9155	0.9119	0.9007	0.8773
50	0.8971	0.8937	0.8851	0.8627
55	0.8783	0.8765	0.8676	0.8474
60	0.8597	0.8582	0.8498	0.8326
65	0.8380	0.8390	0.8310	0.8157
70	0.8157	0.8174	0.8127	0.7986
75	0.7926	0.7929	0.7892	0.7789

Data: July 12,1984

Sample: $BaSO_4$ Panel No.5

Reference: Halon calibrated at (45/0) geometry by NBS (Feb. 8,1984)

Location: Infra. Lab.,OSC

Viewing Zenith Angle: 0 deg.

Irradiance Angle: 10-75 deg.

Table 4. Laboratory calibration of Halon panel.

THE REFLECTANCE FACTOR OF HALON PANEL (RAY'S)

Irradiance Angle(deg)	430-470nm	530-570nm	630-670nm	830-870nm
10	0.9965	1.0007	1.0020	1.0042
15	0.9892	0.9949	0.9951	0.9973
20	0.9829	0.9872	0.9888	0.9901
25	0.9741	0.9794	0.9804	0.9816
30	0.9648	0.9702	0.9716	0.9728
35	0.9556	0.9597	0.9618	0.9636
40	0.9442	0.9489	0.9499	0.9515
45	0.9319	0.9368	0.9377	0.9391
50	0.9166	0.9210	0.9231	0.9253
55	0.8991	0.9042	0.9061	0.9073
60	0.8784	0.8832	0.8860	0.8877
65	0.8539	0.8608	0.8633	0.8638
70	0.8221	0.8297	0.8323	0.8343
75	0.7805	0.7872	0.7919	0.7944

Data: July 12,1984

Sample: Halon panel (Ray's)

Reference: Halon calibrated at (45/0) geometry by NBS (Feb.8, 1984)

Location: Infra. Lab.,OSC

Viewing Zenith Angle: 0 deg.

Irradiance angle: 10-75 deg.

$$R_{ref}(45°/0°) = \frac{V_{ref}(45°/0°) \; * \; R_{NBS}(45°/0°)}{V_{NBS}(45°/0°)} \qquad (2)$$

Next, the desired reflectance factor was computed from

$$R_{ref}(\theta/0°) = \frac{V_{ref}(\theta/0°) \; * \; \cos45° \; * \; R_{ref}(45°/0°)}{V_{ref}(45°/0°) \; * \; \cos\theta} \qquad (3)$$

The above steps were repeated for four spectral bandpass filters, each 40 nm wide. The measurement uncertainty was estimated to be less than 1%. A small error in the reflectance factor was also introduced due to the non-uniformity of the panels. In the field the radiance reflected from the panels was averaged over a larger area. This was due to the 15° FOV, as compared to the 1° FOV of the laboratory radiometer. The results of the panel calibration are shown in Table 3 for the BaSO₄ panel, and in Table 4 for Ray Jackson's Halon panel.

Reflectance Data

Both the Barnes data and the panel calibration data were used to determine the reflectance factors of each of the test sites at White Sands. It is noted that the field measurements were taken at several times throughout the morning. Those data taken closest to the time of the Landsat overpass, 11:07:40 MDT, were used in the radiance computations.

Several interpolations had to be made on the laboratory calibration data. The solar zenith angles were first computed for those times at which a field measurement of the sands was taken. The panel reflectance factors of Tables 3 and 4 were next interpolated to find the corresponding reflectance factors at these angles, for the four spectral filters available on Che's radiometer. These wavelengths differ from

those of the Barnes, therefore one more interpolation was necessary. The intermediate computations were used to compute the reflectances for the eight Barnes' wavelengths. (The Barnes' wavelengths correspond to those of the TM, for bands 1-4.)

The reflectance factors of the gypsum are determined from the above computed panel reflectances via Equation (1) above. A summary of this data reduction is given in Table 5. Only the data in channels 1-4 are used here. Reflectance factors are given for pixels 1-16. A schematic of the site, which identifies these pixels is shown in Figure 3.

Radiative Transfer Computations

The mean reflectance values, given in the bold type of Table 5, were used as input to the radiative transfer code. Also input were the atmospheric components listed in Table 2. The usual model assumptions were made for the aerosols. The maximum, minimum, and incremental radial sizes were 5.02, 0.02, and 0.04 μm, respectively. A refractive index of 1.54-0.01i was assumed. The code was run for both a solar zenith angle of 25° and 35°. The output, given in Table 6, is normalized for an exo-atmospheric solar irradiance of 1. After interpolating the data for a solar angle of 29.22° (that corresponding to the time of the overpass) the output is multiplied by the appropiate irradiance value. These final values are given in Table 7. They are the radiances that were incident on the TM sensor, for the morning of July 8.

Summary

Because of instrumentation problems and difficulties in accurately mapping ground reflectance due to the helicopter photography not being

Table 5. Absolute Reflectance of White Sands test sites.

North Site

ABSOLUTE REFLECTANCE

TIME	CH(1)	.	.	.	CH(7)		

BaSO4

TIME	CH(1)						CH(7)
10:52	.957	.952	.939	.915	.858	.839	.715
11:02	.964	.959	.946	.921	.863	.844	.718

ROAD

| 10:54 | .510 | .577 | .619 | .650 | .625 | .527 | .259 |

PIXELS 1-4,8

10:57	.503	.573	.616	.648	.620	.517	.246
10:57	.510	.581	.627	.660	.632	.527	.236
10:58	.515	.584	.629	.661	.631	.525	.244
10:59	.530	.601	.645	.680	.646	.535	.231
11:01	.504	.571	.617	.652	.629	.526	.231

BASO4

| 11:02 | .964 | .959 | .946 | .921 | .863 | .844 | .718 |
| 11:08 | .968 | .963 | .950 | .924 | .866 | .846 | .719 |

PIXELS 7-5

11:04	.475	.538	.579	.610	.589	.492	.233
11:05	.488	.552	.594	.626	.601	.497	.230
11:06	.504	.571	.613	.643	.611	.502	.224

BASO4

| 11:08 | .968 | .963 | .950 | .924 | .866 | .846 | .719 |
| 11:15 | .973 | .968 | .954 | .929 | .869 | .849 | .719 |

PIXELS 9-12

11:08	.488	.555	.599	.630	.605	.501	.230
11:10	.504	.574	.620	.653	.623	.511	.229
11:11	.512	.580	.624	.657	.627	.519	.228
11:12	.526	.597	.643	.676	.637	.520	.213

BASO4

| 11.15 | .973 | .968 | .954 | .929 | .869 | .849 | .719 |
| 11.20 | .976 | .971 | .958 | .932 | .871 | .851 | .720 |

PIXELS 13-16

11.17	.501	.566	.608	.637	.611	.512	.252
11.18	.533	.602	.644	.674	.640	.533	.225
11.19	.511	.581	.624	.656	.631	.526	.228
11.20	.513	.583	.626	.656	.621	.508	.215

CUMULATIVE:

	CH(1)						CH(7)
MEAN	.507	.576	.619	.651	.622	.516	.731
SDEV	.015	.017	.018	.019	.015	.013	

Table 5. Continued

ORIGINAL
OF POOR

South Site

ABSOLUTE REFLECTANCE

TIME   CH(1) . . . CH(7)

Halon

10:58	.965	.968	.970	.971	.973	.974	.980
11:09	.969	.973	.974	.975	.977	.978	.983

1ST SCAN (PIXELS 1-16)

10:59	.489	.551	.599	.642	.625	.500	.233
10:59	.494	.557	.601	.638	.618	.497	.241
11:00	.491	.548	.590	.627	.604	.481	.229
11:00	.468	.529	.573	.612	.591	.468	.229
11:01	.487	.546	.588	.626	.600	.480	.246
11:01	.493	.550	.592	.632	.606	.482	.228
11:02	.509	.572	.615	.653	.630	.508	.251
11:02	.514	.576	.618	.658	.628	.500	.231
11:03	.486	.546	.590	.629	.614	.491	.236
11:04	.503	.567	.611	.650	.634	.519	.256
11:04	.516	.578	.622	.660	.637	.512	.243
11:05	.498	.559	.603	.641	.621	.500	.241
11:05	.510	.572	.616	.654	.624	.492	.228
11:06	.510	.569	.610	.647	.616	.489	.230
11:06	.506	.567	.610	.650	.632	.514	.250
11:07	.503	.561	.603	.643	.622	.500	.250
MEAN	.499	.559	.603	.641	.619	.496	.239
SDEV	.013	.014	.013	.013	.013	.014	.010

Halon

11:16	.972	.975	.976	.977	.980	.980	.986
11:27	.976	.979	.980	.981	.984	.984	.989

2ND SCAN (PIXELS 1-16)

11:16	.492	.552	.594	.634	.619	.499	.247
11:17	.495	.561	.607	.646	.625	.500	.240
11:17	.494	.557	.601	.638	.616	.488	.236
11:18	.493	.555	.601	.640	.621	.494	.239
11:18	.499	.558	.600	.638	.612	.487	.248
11:19	.512	.573	.618	.659	.633	.503	.235
11:19	.508	.571	.614	.653	.629	.502	.238
11:20	.520	.582	.626	.666	.638	.503	.234
11:21	.501	.563	.610	.651	.633	.505	.242
11:21	.521	.587	.633	.673	.654	.527	.250
11:22	.519	.582	.626	.665	.643	.513	.239
11:22	.518	.579	.623	.662	.642	.517	.249
11:23	.520	.584	.630	.670	.639	.500	.229
11:24	.513	.573	.618	.659	.633	.502	.244
11:24	.507	.573	.618	.658	.640	.520	.254
11:25	.514	.574	.616	.655	.630	.501	.250
MEAN	.508	.570	.615	.654	.632	.504	.242
SDEV	.011	.011	.012	.012	.011	.011	.007

Table 5. Continued

Road Site

ABSOLUTE REFLECTANCE
TIME   CH(1) . . . CH(7)

BASO4
| 10:27 | .940 | .935 | .924 | .900 | .846 | .828 | .711 |
| 10:32 | .943 | .939 | .927 | .903 | .849 | .831 | .711 |

1ST DARK AREA
10:28	.445	.495	.529	.553	.540	.472	.235
10:28	.459	.508	.541	.562	.543	.473	.228
10:28	.463	.513	.544	.565	.543	.470	.223
10:29	.458	.509	.543	.564	.543	.470	.224
10:29	.473	.525	.559	.581	.558	.481	.226
MEAN	.459	.510	.543	.565	.545	.473	.227
SDEV	.010	.011	.011	.010	.007	.005	.005

1ST LIGHT AREA
10:29	.516	.580	.623	.656	.607	.480	.178
10:30	.501	.560	.600	.632	.585	.463	.169
10:30	.504	.564	.602	.635	.589	.469	.174
MEAN	.507	.568	.608	.641	.594	.471	.174
SDEV	.008	.010	.013	.013	.012	.009	.004

BASO4
| 10:37 | .947 | .942 | .930 | .906 | .851 | .832 | .712 |
| 10:40 | .949 | .944 | .932 | .908 | .852 | .834 | .712 |

2ND DARK AREA
10:37	.447	.495	.527	.549	.534	.467	.233
10:38	.455	.505	.538	.559	.543	.473	.233
10:38	.457	.506	.538	.560	.541	.469	.224
10:38	.457	.507	.540	.562	.541	.467	.224
10:38	.476	.525	.558	.579	.556	.476	.223
MEAN	.458	.508	.540	.562	.543	.470	.227
SDEV	.011	.011	.011	.011	.008	.004	.005

2ND LIGHT AREA
10:39	.516	.578	.618	.651	.604	.477	.177
10:39	.505	.566	.605	.638	.590	.463	.167
10:40	.504	.561	.597	.628	.583	.464	.172
MEAN	.509	.568	.607	.639	.592	.468	.172
SDEV	.007	.009	.011	.011	.010	.008	.005

BASO4
| 11:38 | .989 | .983 | .969 | .942 | .879 | .859 | .722 |
| 11:42 | .991 | .986 | .972 | .945 | .881 | .860 | .723 |

Road Site. Continued

3RD DARK AREA

11:39	.478	.534	.568	.589	.569	.495	.245
11:39	.479	.534	.569	.591	.567	.488	.233
11:40	.487	.543	.577	.598	.573	.493	.236
11:40	.485	.542	.577	.598	.571	.490	.233
11:40	.499	.554	.587	.608	.580	.495	.232
MEAN	.486	.541	.576	.597	.572	.492	.236
SDEV	.008	.008	.008	.008	.005	.003	.005

3RD LIGHT AREA

11.41	.540	.608	.651	.682	.629	.498	.189
11.41	.530	.597	.639	.669	.614	.481	.176
11.42	.530	.598	.639	.667	.613	.485	.181
MEAN	.533	.601	.643	.673	.619	.488	.182
SDEV	.006	.006	.007	.008	.009	.009	.006

Table 6. Herman Code Output

WAV	τ_{Mie}	τ_{Ray}	τ_{oz}	θ_z	ρ	E_{dir}	E_{dif}	L_{path}	L_t
0.486	0.0864	0.1421	0.0055	25	0.507	0.7001	0.1519	0.0246	0.1334
					0.499		0.1504	0.0244	0.1313
0.486	0.0864	0.1421	0.0055	35	0.507	0.6156	0.1417	0.0223	0.1190
					0.499		0.1404	0.0222	0.1172
0.571	0.0777	0.0735	0.0232	25	0.576	0.7477	0.1113	0.0134	0.1457
					0.559		0.1088	0.0133	0.1413
0.571	0.0777	0.0735	0.0232	35	0.576	0.6621	0.1028	0.0121	0.1299
					0.559		0.1006	0.0120	0.1260
0.661	0.0706	0.0406	0.0114	25	0.619	0.7916	0.9078	0.0080	0.1618
					0.603		0.8880	0.0079	0.1574
0.661	0.0706	0.0406	0.0114	35	0.619	0.7053	0.8337	0.0072	0.1447
					0.603		0.8160	0.0071	0.1407
0.838	0.0605	0.0156	0.0013	25	0.651	0.8321	0.6780	0.0033	0.1759
					0.641		0.6683	0.0032	0.1730
0.838	0.0605	0.0156	0.0013	35	0.651	0.7453	0.6182	0.0030	0.1578
					0.641		0.6095	0.0029	0.1552

where

E_{dir} The downward direct solar irradiance at the ground, $\cos\theta_z$ * $\exp(-\tau_{ext} \sec\theta_z)$.

E_{dif} The downward diffuse solar irradiance at the ground.

L_{path} The upward path radiance at the TM, $L_T - (E_{dir}+E_{dif})$ * $\exp(-\tau_{ext} \sec 5^\circ)\rho/\pi$

L_t The total radiance at the TM at a 5° nadir angle.

Note all irradiance and radiance values are normalized for an exo-atmospheric solar irradiance of 1.

Table 7. Computed radiance at Landsat sensors.

$$L \ (mW/cm^2 sr \ \mu m)$$

Band	North Site	South Site
1	23.18	22.82
2	25.13	24.37
3	23.82	23.17
4	17.64	17.35

vertical, the results of the July 8, 1984 measurement will have high uncertainties associated with them. However, the measurement attempt was worthwhile because of the experience gained in instrument operation and measurement.

There are still a few remaining computations to be made with the July 8th data. Only a few discrete points of data were taken at the pixel centers of the two test sites. We are currently exploring the usage of the aerial photography (the slide imagery which has been scanned) to better characterize the reflectance of the area. The radiosonde and humidity data will also be looked at. Once the optical depth component τ_{H2O} can be determined, the Herman code will be rerun to account for atmospheric water vapor in band 4. The diffuse to direct data will be compared with the Herman code output. Finally, it remains to inspect the Landsat imagery, identify our test site, and compute incident radiance, as determined from the pre-flight data. A comparison can then be made of our in-flight calibration, to that made based upon pre-flight data and the internal calibrator data. The calibrations of bands 5 and 7 will not be investigated for this date. No atmospheric data are available at these wavelengths and the optical depth components cannot be computed. The Castle spectropolarimeters will be equipped with a filter set which will allow us, in the future, to do calibrations in the short wave infrared.

References

1. Neckel, H. and D. Labs. "Improved data of solar spectral irradiance from 0.33 to 1.25 μm". Solar Physics, Vol. 74, p. 231, 1981.

2. Palmer, James M. "Effective bandwidths for Landsat-4 and Landsat-4' multispectral scanner and thematic mapper subsystems". IEEE trans, Geoscience and Remote Sensing, Vol. GE-22, p.336-338, 1984.

APPENDIX A

Reflectance

The nomenclature, measuring geometry, and techniques associated with determining the reflectance of a given surface are quite varied. With this in mind, the technical basis of our measurements at White Sands is presented here. We are interested in the directional properties, as well as the magnitude, of the reflectance at the field site, for this reason we determine the reflectance factor. Reflectance factor and other quantities are defined below. A spectral dependance is assumed for each quantity. All of our reflectance measurements are made with finite spectral bandwidths. These are, in general, the 40 nm bandwidths of a laboratory radiometer, or those bandwidths associated with the Thematic Mapper and the Barnes modular multiband radiometer.

Definitions and Nomenclature

Reflectance Factor, $R(\theta,\phi;\theta',\phi')$ (unitless). Ratio of the flux reflected by a sample surface to that which would be reflected into the same beam geometry by a lossless, lambertian surface which is identically irradiated. Thus,

$$R(\theta,\phi;\theta',\phi') = \frac{\displaystyle\int_{IFOV} L_t(\theta',\phi')\cos\theta' \, \sin\theta' \, d\theta' \, d\phi'}{\displaystyle\int_{IFOV} L_p(\theta',\phi')\cos\theta' \, \sin\theta' \, d\theta' \, d\phi'} \qquad (1)$$

is the reflectance factor measured with a detector having a given

instantaneous field of view (IFOV). L_t is the radiance reflected off the sample target, and L_p is the radiance reflected off a perfect (lossless), diffuse surface. The incident beam originates from (θ,ϕ), and the reflected beam is viewed in the direction (θ',ϕ').

Reflectance ρ (unitless). Ratio of the reflected flux to the incident flux. When referring to this parameter one needs to specify if the flux is integrated over the reflecting hemisphere, or if the reflected flux is measured within a given cone angle. The hemispherical reflectance can be related to the reflectance factor by

$$\rho = \int_{2\pi} \int_{\pi/2} L_t(\theta',\phi')\cos\theta' \sin\theta' \, d\theta' \, d\phi'/E \qquad (2)$$

$$= R(\theta,\phi;2\pi)$$

where E is the incident irradiance, generally from a well collimated beam. It is computed from

$$E = \int \int_{\omega} L_t(\theta,\phi)\cos\theta \sin\theta \, d\theta \, d\phi \qquad (3)$$

Note the integration is over the solid angle $d\omega = \sin\theta \, d\theta \, d\phi$.

Bidirectional Reflectance Distribution Function (BRDF), f (sr^{-1}). The ratio of the radiance reflected in the direction (θ',ϕ') to the total irradiance on the surface from the direction (θ,ϕ).

$$f(\theta,\phi;\theta',\phi') = L_t(\theta',\phi')/E \qquad (4)$$

The quantity $R(\theta,\phi;2\pi)$ is equivalent to ρ. The 2π denotes that the reflectance factor has been integrated over a hemisphere. $R(\theta;d)$, or $R(\theta/d)$, is an equivalent description, the "d" denoting that diffuse reflectance has been accounted for. Even when an integration is not

implied, the symbols ϕ and ϕ' are often dropped for simplicity (as is true for any of the above parameters).

Choice of the Reflectance Factor

In calibrating the TM we are interested in knowing the radiance reflected from the gypsum sands into a number of discrete angles. This allows both the directly and diffusely reflected solar radiation to be accurately characterized. Such a complete BRDF measurement is, however, both time consuming and difficult to measure. The equipment required is relatively complex, and there are difficulties associated with measuring the incident irradiance. Instead we have chosen to characterize the gypsum by the reflectance factor $R(\theta_z;0^\circ)$. This accurately describes the flux that is directly reflected towards the Landsat sensors. As the gypsum sands are not truely lambertian, some error is incured in not computing the full BRDF. Without the BRDF data, a lambertian surface is assumed. Thus an overestimate is made in the radiance not directly reflected towards the TM. Due to atmospheric multiple scattering in the atmosphere, some of this flux edventually reaches the sensors. This is the diffuse component of the radiance. The error made in predicting this term increases with increased multiple scattering, and with departure from a lambertian behavior. Even so, the usage of the reflectance factor is justified. This is because the radiance received at the TM is dominated by the direct component, and multiple scattering is minimal for clear atmospheric conditions.

Calibrating the Field Reference

The reflectance factor is measured with respect to a reference panel which is calibrated in the laboratory to account for its non-ideal characteristics. The calibration procedure was briefly described in the body of the report. Here a development of the equations used in the two step calibration procedure is given.

To begin with, it is assumed that a laboratory standard is available. In our case a 50 mm diameter Halon disc was used which had been calibrated by NBS to determine $R_{NBS}(45°;0°)$. The fictional parameter $V_p(45°;0°)$ is thereby computed:

$$V_p(45°;0°) = \frac{V_{NBS}(45°;0°)}{R_{NBS}(45°;0°)} \tag{5}$$

This is the voltage that would have been measured had a perfect (lossless) lambertian surface been present.

Using the above, the reflectance factor of the reference panel is found for the same geometry:

$$R_{ref}(45°;0°) = \frac{V_{ref}(45°;0°)}{V_p(45°;0°)} \tag{6}$$

$$= \frac{V_{ref}(45°;0°) \star R_{NBS}(45°;0°)}{V_{NBS}(45°;0°)}$$

In the next phase of calibration, the reflectance factor measurements are made at the angle of interest, θ. For the ideal lambertian surface the detector response at angle θ is easily predicted from the response at 45°. Such a surface reflects radiance uniformly into the upper hemisphere, thereby reflecting a factor of $1/\pi$ of the incident irradiance. Thus, for this perfect ($\rho=1$) lambertian surface, illuminated with a beam of irradiance $E(\theta)$, the following relationships

hold:

$$V_p(45°;0°) = R * E(45°) \, \rho/\pi = R * E_o \, \cos45°/\pi \qquad (7)$$

$$V_p(\theta;0°) = R * E(\theta) \, \rho/\pi = R * E_o \, \cos\theta/\pi \qquad (8)$$

$$= \frac{V_p(45°;0°) * \cos\theta}{\cos45°}$$

The detector is assumed to have a given response, R, to the incoming radiance. This latter result is now substituted into the equation for $R_{ref}(\theta;0°)$, to yield the final, desired result:

$$R_{ref}(\theta;0°) = \frac{V_{ref}(\theta;0°)}{V_p(\theta;0°)} \qquad (9)$$

$$= \frac{V_{ref}(\theta;0°) * \cos45°}{V_p(45°;0°) * \cos\theta}$$

$$= \frac{V_{ref}(\theta;0°) * \cos45° * R_{ref}(45°;0°)}{V_{ref}(45°;0°) * \cos\theta}$$

APPENDIX B

Radiosonde and atmospheric data for July 8th, as provided by the
Atmospheric Sciences Laboratory, White Sands Missle Range.

PROJECT SURFACE OBSERVATION

STATION __CHUCK SITE__

X= __32° 54'__ Y= __106° 18'__ H= __3912.75f__

MISSION CODE __LANDSAT 5__

DATE __DAY 08__ __MONTH 07__ __YEAR 84__

TIME M D J	PRESSURE mbs	TEMPERATURE °F	°C	DEW POINT °F	°C	RELATIVE HUMIDITY %	DENSITY gm/m³	WIND DIRECTION degs Tn	WIND SPEED kts	CHARACTER kts	VISIBILITY
0730	883.8	68.4	20.2	54.3	12.4	61	1042	105	01		40
0930	883.4	81.0	27.2	56.1	13.4	42	1019	095	01		40
0945	883.4	83.3	28.5	55.2	12.9	38	1015	100	01		40

REMARKS

CLOUDS

	1st LAYER			2nd LAYER			3rd LAYER		
	AMT	TYPE	HGT	AMT	TYPE	HGT	AMT	TYPE	HGT
							1	Ci	25000
							2	Ci	25000
							2	Ci	25000

OBSTRUCTIONS TO VISIBILITY

PSYCHROMETRIC COMPUTATION

TIME:	0730	0930	0945
DRY BULB TEMP.	20.2	27.2	28.5
WET BULB TEMP.	15.2	18.0	18.1
WET BULB DEPR.	5.0	9.2	10.4
DEW POINT	12.4	13.4	12.9
RELATIVE HUMID.	61	42	38

R Savage
OBSERVER

_____ VERIFIER

PROJECT SURFACE OBSERVATION

MISSION CODE LANDSAT-5

STATION CHUCK SITE

DATE 08 DAY 07 MONTH 84 YEAR

X= 32°54' Y= 106°18' H= 3912.75ft

TIME MDT	PRESSURE mbs	TEMPERATURE °F	TEMPERATURE °C	DEW POINT °F	DEW POINT °C	RELATIVE HUMIDITY %	DENSITY gm/m³	WIND DIRECTION degs Tn	WIND SPEED kts	WIND CHARACTER kts	VISIBILITY
1000	883.3	84.4	29.1	55.2	12.9	37	1012	090	02		40
1015	883.2	86.0	30.0	59.0	15.0	40	1009	095	03		40
1030	883.2	86.4	30.2	59.2	15.1	40	1008	080	05		40

CLOUDS

1st LAYER AMT	TYPE	HGT	2nd LAYER AMT	TYPE	HGT	3rd LAYER AMT	TYPE	HGT
1	Cu	6000	0	AC	12000	2	Ci	25000
1	Cu	6000	0	AC	12000	2	Ci	25000
2	Cu	6000	0	AC	12000	2	Ci	25000

OBSTRUCTIONS TO VISIBILITY

REMARKS

PSYCHROMETRIC COMPUTATION

TIME:	1000	1015	1030
DRY BULB TEMP.	29.1	30.0	30.2
WET BULB TEMP.	18.3	19.7	19.8
WET BULB DEPR.	10.8	10.3	10.4
DEW POINT	12.9	15.0	15.1
RELATIVE HUMID.	37	40	40

R. Savage
OBSERVER

_____
VERIFIER

Supersedes AFSEL-BL-HT-MS Form 12, 28 Aug 72 and all project surface observation forms, except DIVAD Surface Observation for.

DELAS-MS-MT-WS FORM 12
01 NOV 1980

PROJECT SURFACE OBSERVATION

MISSION CODE LANDSAT-5

STATION CHUCK SITE

DATE 08 DAY 07 MONTH 84 YEAR

X = 32°54' Y = 106°18' H = 3912.75ft

TIME M D T	PRESSURE mbs	TEMPERATURE °F	°C	DEW POINT °F	°C	RELATIVE HUMIDITY %	DENSITY gm/m³	WIND DIRECTION degs Tn	SPEED kts	CHARACTER kts	VISIBIL-ITY
1045	883.2	86.9	30.5	58.8	14.9	39	1007	095	04		40
1100	883.1	88.3	31.3	58.5	14.7	36	1005	095	04		40
1107	883.0	90.0	32.2	57.9	14.4	34	1002	100	04		40

CLOUDS

OBSTRUCTIONS TO VISIBILITY	1st LAYER AMT	TYPE	HGT	2nd LAYER AMT	TYPE	HGT	3rd LAYER AMT	TYPE	HGT
	2	Cu	6000	0	AC	12000	2	Ci	25000
	2	Cu	6000	0	AC	12000	2	Ci	25000
	2	Cu	6000	0	AC	12000	2	Ci	25000

REMARKS

PSYCHROMETRIC COMPUTATION

TIME:	1045	1100	1107
DRY BULB TEMP.	30.5	31.3	32.2
WET BULB TEMP.	19.8	19.9	20.0
WET BULB DEPR.	10.7	11.4	12.2
DEW POINT	14.9	14.7	14.4
RELATIVE HUMID.	39	36	34

R. Savage
OBSERVER

_____
VERIFIER

DELAS-MS-MT-WS FORM 12
01 NOV 1980

Supersedes AMSEL-BL-MT-WS Form 12, 28 Aug 72 and all project surface observation forms, except DIVAD Surface Observation for.

PROJECT SURFACE OBSERVATION

MISSION CODE __LANDSAT-5__

STATION __CHUCK SITE__

X= __32°54'__   Y= __106°18'__   H= __3912.75ft__

DATE __03__ DAY __07__ MONTH __84__ YEAR

TIME MDT	PRESSURE mbs	TEMPERATURE °F	°C	DEW POINT °F	°C	RELATIVE HUMIDITY %	DENSITY gm/m³	WIND DIRECTION degs Tn	SPEED kts	CHARACTER kts	VISIBILITY
1115	882.9	92.1	33.4	57.6	14.2	31	998	100	03		40
1130	882.8	95.0	35.0	57.0	13.9	28.	993	095	04		40

CLOUDS

	1st LAYER			2nd LAYER			3rd LAYER		
	AMT	TYPE	HGT	AMT	TYPE	HGT	AMT	TYPE	HGT
	2	Cu	6000	0	AC	12000	2	Ci	25000
	2	Cu	6000	0	AC	12000	2	Ci	25000

OBSTRUCTIONS TO VISIBILITY

REMARKS

PSYCHROMETRIC COMPUTATION

TIME:	1115	1130
DRY BULB TEMP.	33.4	35.0
WET BULB TEMP.	20.2	20.5
WET BULB DEPR.	13.2	14.5
DEW POINT	14.2	13.9
RELATIVE HUMID.	31	28

(signature) R. Savage

OBSERVER

VERIFIER

Supersedes ANSEL-GL-MT-WS Form 12, 28 Aug 72 and all project surface observation forms, except DIVAD Surface Observation for.

STAT ALTITUDE ___ ___ FEET MSL
JULY 5-
ASCENSION NO. ___

SIGNIFICANT LEVEL DATA
___
WHITE SANDS

GEODETIC COORDINATES
32.___ LAT DEG
106.37___ LON DEG

PRESSURE MILLIBARS	GEOMETRIC ALTITUDE MSL FEET	TEMPERATURE AIR DEGREES CENTIGRADE	DEWPOINT DEGREES CENTIGRADE	REL.HUM. PERCENT
___	3999.0	26.2	12.2	40.0
871.1	4315.5	24.3	3.7	37.0
___	4015.7	22.2	9.1	___
___	4247.2	20.0	7.4	44.0
747.1	5071.9	15.8	5.1	49.0
725.5	5483.5	14.0	2.0	47.0
___	10471.2	11.5	2.5	54.0
___	11194.7	9.3	1.7	___
___	12415.9	6.3	-1.6	52.0
___	13144.0	4.0	-1.6	57.0
___	13916.2	3.0	-10.4	36.0
___	14294.0	3.0	-14.5	25.0
___	15551.0	1.5	-15.0	23.0
558.3	16594.4	-.1	-20.7	17.0
___	18541.4	-4.5	-24.5	12.0
___	19407.2	-7.1	-26.7	19.0
425.0	27035.7	-7.3	-23.1	17.0
___	25044.5	-17.0	-34.1	20.0
___	27746.0	-24.4	-40.8	23.0
___	31941.0	-35.3	-43.0	21.0
___	37510.5	-36.4	-50.7	21.0
___	34640.5	-39.2	-52.0	24.0
___	36576.6	-42.9		
___	38554.4	-49.1		
___	40911.8	-53.9		
170.2	44473.2	-60.7		
___	44965.7	-64.0		
___	49249.5	-57.8		
___	51415.1	-70.3		
___	54249.5	-71.2		
___	56096.5	-55.8		
___	60091.7	-54.7		
___	56225.4	-51.5		
___	65292.5	-55.7		
___	71262.3	-52.8		
___	75264.4	-52.4		
___	79521.3	-51.7		
___	84441.6	-51.7		
___	89425.3	-46.1		
___	94559.2	-22.2		

SIGNIFICANT LEVEL DATA
1990?33cc
WHITE SANDS

GEODETIC COORDINATES
32.63043 LAT DEG
106.37053 LON DEG

STATION ALTITUDE 3753.0 FEET MSL
6 JULY 84
ASCENSION NO. 356   1300 HRS MST

PRESSURE MILLIBARS	GEOMETRIC ALTITUDE MSL FEET	TEMPERATURE AIR DEGREES CENTIGRADE	DEW POINT	REL.HUM. PERCENT
12.6	27121.1	-43.1		

STATION ALTITUDE 5296.0 FEET MSL
6 JULY 84   0850 HRS MST
ASCENSION NO. 256

UPPER AIR DATA
1980030106
WHITE SANDS

GEODETIC COORDINATES
32.40063 LAT DEG
106.37233 LON DEG

GEOMETRIC ALTITUDE MSL FEET	PRESSURE MILLIBARS	TEMPERATURE AIR DEGREES CENTIGRADE	DEWPOINT DEGREES CENTIGRADE	REL.HUM. PERCENT	DENSITY GM/CUBIC METER	SPEED OF SOUND KNOTS	WIND DATA DIRECTION DEGREES(TN)	SPEED KNOTS	INDEX OF REFRACTION
		20.9	1.2	41.0	1017.5	675.9	.0	.0	1.000225
		20.7	12.0	69.9	1014.5	676.3	170.0	.1	1.000243
		23.9	6.6	38.3	1010.1	673.1	152.7	1.5	1.000274
		22.7	5.1	41.9	994.2	671.9	190.9	5.2	1.000272
		22.0	2.7	42.5	981.2	671.0	190.2	10.4	1.000263
		21.5	1.6	43.0	954.7	670.2	191.6	11.7	1.000243
		20.6	7.1	43.6	952.0	657.4	192.4	11.6	1.000259
		19.3	7.1	44.2	934.2	653.4	175.0	9.6	1.000256
		18.0	5.7	45.7	915.5	657.0	201.7	7.5	1.000250
		17.4	6.0	47.1	917.1	565.0	204.5	7.4	1.000245
		16.4	5.4	45.5	900.0	554.2	206.5	7.1	1.000241
		15.1	4.2	46.2	856.5	552.3	205.1	5.6	1.000235
		14.0	1.9	47.1	874.4	661.4	175.5	4.9	1.000230
		12.7	1.7	50.6	844.5	550.0	165.2	5.4	1.000227
		11.4	1.5	54.2	857.8	653.3	125.4	4.9	1.000224
		9.9	1.1	56.5	841.0	555.7	105.4	7.2	1.000221
		8.5	1.4	56.5	830.7	555.1	24.5	9.9	1.000217
		7.3	.4	51.3	910.3	553.6	89.1	10.7	1.000213
		5.0	-1.3	52.0	808.1	552.1	84.1	12.3	1.000209
		4.5	-1.5	55.2	797.7	550.2	35.3	13.6	1.000205
		3.2	-1.2	55.8	786.0	549.0	86.7	14.8	1.000196
		2.7	-11.1	26.6	775.5	648.1	79.1	14.2	1.000185
		2.0	-14.7	27.3	765.0	547.4	79.7	15.5	1.000177
		1.7	-14.2	26.9	756.2	545.6	109.4	13.2	1.000172
		.7	-15.5	24.1	736.2	545.3	118.4	13.5	1.000163
		-.7	-17.9	19.6	724.4	645.3	127.2	16.2	1.000165
		-1.9	-21.5	19.6	712.1	643.3	135.0	15.0	1.000162
		-2.6	-20.6	19.0	701.5	641.0	138.0	15.9	1.000159
		-3.1	-25.5	15.0	593.1	541.6	141.6	14.5	1.000155
		-4.4	-24.5	19.0	680.0	560.3	144.9	14.5	1.000154
		-5.7	-24.5	19.0	670.0	638.7	145.8	13.1	1.000151
		-6.4	-25.7	19.0	661.7	537.1	145.5	13.5	1.000149
		-7.4	-27.4	17.0	652.1	535.8	144.5	14.7	1.000140
		-8.0	-24.0	17.2	652.2	535.5	148.7	15.5	1.000143
		-9.1	-26.2	17.2	637.5	534.4	152.7	15.5	1.000141
		-9.5	-29.2	17.4	637.5	533.3	157.3	17.7	1.000175
		-10.3	-29.7	15.8	599.0	671.7	160.4	18.9	1.000135
		-11.4	-31.4	15.0	526.0	580.4	152.4	19.6	1.000134
		-12.5	-31.1	15.1	579.7	529.1	151.9	18.4	1.000132

STATION ALTITUDE - ... FEET MSL
1 JULY 8..
ASCENSION NO. ...

UPPER AIR DATA
...
WHITE SANDS

GEODETIC COORDINATES
32.43043 LAT DEG
106.37933 LON DEG

GEOMETRIC ALTITUDE MSL FEET	PRESSURE MILLIBARS	TEMPERATURE AIR DEGREES CENTIGRADE	DEW POINT DEGREES CENTIGRADE	REL.HUM. PERCENT	DENSITY GM/CUBIC METER	SPEED OF SOUND KNOTS	WIND DATA DIRECTION DEGREES(TRUE)	SPEED KNOTS	INDEX OF REFRACTION

STATION ALTITUDE 3970.00 FEET MSL
2 JULY 84   0600 HRS MST
ACCESSION NO. 256

UPPER AIR DATA
1800723365
WHITE SANDS

SEODETIC COORDINATES
32.6043 LAT DEG
135.37053 LON DEG

GEOPOTENTIAL ALTITUDE MSL FEET	PRESSURE MILLIBARS	TEMPERATURE AIR DEGREES CENTIGRADE	DEWPOINT DEGREES CENTIGRADE	REL.HUM. PERCENT	DENSITY GM/CUBIC METER	SPEED OF SOUND KNOTS	WIND DATA DIRECTION DEGREES(TN)	WIND DATA SPEED KNOTS	INDEX OF REFRACTION
43500.0	173.6	-59.1			297.5	559.7	346.9	8.5	1.000046
44000.0	171.1	-59.1			292.3	553.3	331.9	9.0	1.000043
44500.0	168.4	-61.5			276.4	557.4	324.7	10.9	1.000042
45000.0	164.4	-61.9			270.5	555.6	324.6	12.7	1.000060
45500.0	160.2	-62.3			264.7	565.7	342.2	13.9	1.000059
46000.0	156.4	-62.9			250.1	554.7	356.6	16.6	1.000058
46500.0	152.0	-63.6			257.5	554.0	17.5	14.9	1.000065
47000.0	148.6	-64.1			249.2	563.1	32.0	14.6	1.000055
47500.0	145.2	-65.1			247.0	552.0	45.8	14.2	1.000054
48000.0	141.6	-65.7			235.0	550.2	25.3	13.7	1.000053
48500.0	135.1	-66.7			237.0	559.6	57.4	13.5	1.000052
49000.0	134.7	-67.5			228.1	553.7	73.5	11.7	1.000051
49500.0	131.1	-68.1			222.2	557.8	81.0	9.8	1.000050
50000.0	128.1	-68.7			218.2	557.0	84.7	7.8	1.000049
50500.0	124.6	-69.3			217.3	555.3	92.0	6.3	1.000043
51000.0	121.7	-69.6			208.5	555.5	104.5	5.9	1.000036
51500.0	118.7	-70.3			267.8	554.8	112.9	7.8	1.000045
52000.0	115.7	-70.5			196.8	554.7	115.8	9.6	1.000044
52500.0	112.6	-70.0			197.7	554.5	116.0	11.0	1.000043
53000.0	109.9	-70.7			189.1	554.3	115.5	11.6	1.000042
53500.0	107.1	-70.8			184.5	554.1	114.8	12.2	1.000041
54000.0	104.4	-71.0			170.2	553.4	115.3	12.8	1.000040
54500.0	101.9	-71.1			175.5	553.8	115.9	13.5	1.000037
55000.0	99.4	-70.3			170.9	554.1	117.7	14.9	1.000033
55500.0	96.6	-69.7			165.7	555.7	110.2	15.1	1.000037
56000.0	94.3	-68.5			160.7	557.3	120.5	15.5	1.000035
56500.0	92.0	-67.4			156.8	558.7	122.6	15.0	1.000035
57000.0	89.7	-66.2			151.1	549.6	123.0	14.2	1.000034
57500.0	87.6	-66.0			146.5	552.0	124.0	13.3	1.000033
58000.0	85.3	-63.7			142.1	543.6	125.2	11.6	1.000032
58500.0	83.2	-64.7			139.5	553.5	124.5	9.8	1.000031
59000.0	81.2	-64.0			135.8	543.4	102.7	7.7	1.000030
59500.0	79.1	-64.1			152.1	553.2	75.2	7.8	1.000029
60000.0	77.3	-64.2			128.2	553.1	75.2	13.1	1.000029
60500.0	75.4	-64.5			125.8	552.7	77.1	18.3	1.000025
61000.0	73.4	-64.6			122.3	562.6	83.4	21.0	1.000027
61500.0	71.6	-64.0			116.7	562.6	88.2	25.6	1.000027
62000.0	70.0	-64.7			117.3	552.5	94.1	24.9	1.000025
62500.0	68.2	-64.2			113.2	553.1	100.3	24.6	1.000025
63000.0	66.6	-63.8			110.2	563.7	103.5	24.5	1.000025

STATION ALTITUDE 36.9.00 FEET MSL
6 JULY 54   0800 HRS MST
ASCENSION NO. 250

UPPER AIR DATA
1600 HRS
WHITE SANDS

GEODETIC COORDINATES
32.43063 LAT DEG
106.37953 LON DEG

GEOMETRIC ALTITUDE MSL FEET	PRESSURE MILLIBARS	TEMPERATURE AIR / DEWPOINT DEGREES CENTIGRADE	REL.HUM. PERCENT	DENSITY GM/CUBIC METER	SPEED OF SOUND KNOTS	WIND DATA DIRECTION DEGREES(TN)	SPEED (KNOTS)	INDEX OF REFRACTION
				108.0	564.3	105.0	24.5	1.000024
				105.1	564.9	106.1	24.7	1.000023
				102.3	555.3	103.4	25.2	1.000023
				90.5	565.2	99.0	25.6	1.000022
				97.0	565.3	99.7	25.2	1.000022
				94.4	567.6	92.2	27.4	1.000021
				91.8	558.6	81.4	27.5	1.000021
				88.3	562.5	81.5	27.6	1.000020
				86.9	570.5	85.5	25.8	1.000019
				84.5	571.4	94.4	25.0	1.000018
				82.3	572.4	99.7	25.8	1.000018
				80.1	573.1	99.2	25.0	1.000017
				78.3	572.7	98.5	25.2	1.000017
				76.5	572.4	99.5	25.0	1.000017
				74.5	571.5	98.5	25.0	1.000017
				72.5	571.5	96.1	25.0	1.000016
				70.5	571.0	99.0	25.9	1.000016
				69.5	572.4	97.9	25.9	1.000015
				67.3	573.0	101.5	25.7	1.000015
				66.0	573.1	105.2	25.6	1.000015
				64.3	574.7	106.5	24.0	1.000014
				62.5	575.5	105.7	25.3	1.000014
				61.0	575.2	105.8	23.5	1.000013
				59.4	577.0	102.7	23.7	1.000013
				57.9	577.7	99.5	24.5	1.000013
				56.4	578.3	99.8	25.4	1.000012
				55.1	578.1	99.3	25.2	1.000012
				53.9	578.0	97.9	25.3	1.000012
				52.6	579.1	96.9	25.4	1.000012
				51.4	578.4	98.5	21.5	1.000011
				50.2	578.4	85.4	20.8	1.000011
				49.0	577.7	95.3	20.9	1.000011
				47.9	577.5	96.9	22.3	1.000011
				46.7	577.7	94.4	23.8	1.000010
				44.5	578.1	92.5	25.6	1.000011
				43.5	578.4	55.1	23.4	1.000011
				42.5	578.8	34.4	24.1	1.000011
				41.5	578.8	91.0	29.7	1.000011
				40.6	577.1	83.2	32.5	1.000010

STATION ALTITUDE 3969.05 FEET MSL

6 JULY 84

ASCENSION NO. 256

UPPER AIR DATA
TOOTOOSEE
WHITE SANDS

GEODETIC COORDINATES
32.4004 LAT DEG
106.37035 LON DEG

GEOMETRIC ALTITUDE MSL FEET	PRESSURE MILLIBARS	TEMPERATURE AIR DEGREES CENTIGRADE	DEWPOINT DEGREES CENTIGRADE	REL.HUM. PERCENT	DENSITY GM/CUBIC METER	SPEED OF SOUND KNOTS	WIND DATA DIRECTION DEGREES(TN)	SPEED KNOTS	INDEX OF REFRACTION
					30.5	579.3	94.4	35.7	1.000006
					39.5	579.5	35.4	37.9	1.000009
					37.7	579.8	36.5	40.1	1.000005
					36.7	580.7	87.5	42.2	1.000008
					35.8	581.7	88.0	43.9	1.000005
					34.9	582.6	87.4	44.7	1.000008
					37.9	583.5	85.9	44.8	1.000005
					37.1	584.4	55.5	45.4	1.000007
					37.2	585.3	84.3	45.0	1.000007
					37.4	585.2	85.1	46.7	1.000007
					30.5	587.1	96.1	47.3	1.000007
					40.3	587.7	35.2	47.9	1.000005
					29.1	588.2	86.1	48.5	1.000005
					34.4	593.7	96.1	48.3	1.000005
					27.7	539.3	85.3	47.0	1.000005
					27.1	589.8	84.5	45.7	1.000005
					24.4	590.4	84.2	44.9	1.000005
					25.8	590.9	84.5	45.3	1.000005
					25.2	591.5	84.9	45.6	1.000005
					24.5	571.7	95.5	46.0	1.000005
					24.0	592.1	37.7	45.4	1.000005
					25.5	592.2	89.8	45.8	1.000005
					22.0	592.5	91.3	47.4	1.000005
					22.4	592.7	93.7	45.7	1.000005
					21.4	593.0	94.5	45.8	1.000004
					20.7	593.2	96.9	44.9	1.000005
					20.4	593.5			1.000005
					20.4	593.7			1.000005
					20.5	593.9			1.000004
					10.5	594.2			1.000004
					10.1	594.4			1.000004
					19.6	594.7			1.000004

STATION ALTITUDE 1272.0 FEET MSL   FOR SIGNIFICANT LEVEL DATA   GEODETIC COORDINATES
8 JULY 84   1000 MST   32.45743 LAT DEG
ASCENSION NO. 530   WHITE SANDS   106.37033 LON DEG

GEOPOTENTIAL ALTITUDE DECAMETERS	WIND DATA				DEW PT DEP DEG C	TEMPERATURE AIR DEG C	PRESSURE MILLIBARS
	DIRECTION DEG (TN)	SPEED MPS	N-S MPS	E-W MPS			
1005.	9999.**	9999.**	-9999.**	-9999.**	99	-40.1	1.240+1
1307.	65.	34.	-2.	-27.	99	-42.5	1.650+1
1442.	80.	24.	-2.	-24.	99	-45.1	2.000+1
1563.	90.	11.	-1.	-11.	99	-51.7	2.400+1
1619.	95.	11.	1.	-11.	99	-53.4	3.000+1
1653.	100.	11.	2.	-11.	99	-52.8	3.590+1
1654.	95.	11.	2.	-11.	99	-53.1	4.650+1
1692.	95.	14.	-1.	-14.	99	-56.7	5.000+1
1795.	87.	14.	1.	-13.	99	-51.3	5.340+1
1463.	94.	11.	2.	-5.	99	-54.7	7.000+1
1753.	160.	6.	7.	-7.	99	-58.6	8.520+1
1667.	117.	7.	3.	-7.	99	-71.2	1.000+2

** WIND DATA NOT COMPUTED DUE TO MISSING RAW AZIMUTH AND ELEVATION ANGLES.

STATION ALTITUDE 3938.0 FEET MSL
6 JULY 84
ASCENSION NO. 255

MANDATORY LEVELS
18002286
WHITE SANDS

GEODETIC COORDINATES
32.43063 LAT DEG
106.37733 LON DEG

PRESSURE	GEOPOTENTIAL	TEMPERATURE		REL.HUM.	WIND DATA	
		AIR	DEWPOINT		DIRECTION	SPEED
MILLIBARS	FEET	DEGREES CENTIGRADE		PERCENT	DEGREES(TN)	KNOTS
850.0	5715.	20.7	9.1	42.	190.9	7.1
800.0	6740.	20.2	7.6	44.	193.9	10.8
750.0	8555.	15.1	5.7	49.	205.4	7.0
700.0	10467.	11.5	2.5	54.	124.9	4.5
650.0	12451.	6.1	-1.5	53.	84.1	12.3
600.0	14517.	2.5	-16.7	27.	101.1	13.4
550.0	16911.	-1.9	-21.5	19.	137.4	15.7
500.0	19589.	-7.1	-26.7	17.	143.7	14.6
450.0	22565.	-10.9	-30.0	18.	152.7	19.8
400.0	25902.	-17.0	-34.1	21.	150.4	15.3
350.0	28243.	-23.5	-40.0	20.	147.8	10.2
300.0	31875.	-33.7	-48.0	21.	92.5	4.5
250.0	35090.	-42.9			22.5	9.1
200.0	40411.	-53.0			359.4	17.7
175.0	43539.	-59.5			341.2	9.5
150.0	46717.	-64.0			27.3	14.9
125.0	50838.	-69.2			90.3	5.3
100.0	54477.	-71.2			117.1	14.4
90.0	59159.	-64.1			65.1	7.3
70.0	61788.	-66.7			53.3	25.0
60.0	64987.	-61.8			99.1	25.6
50.0	68442.	-56.7			90.4	26.0
40.0	73275.	-55.4			105.5	24.9
30.0	79343.	-53.4			95.5	21.2
25.0	83211.	-52.0			84.5	35.5
20.0	86062.	-46.1			85.7	47.2
15.1	94955.	-41.7			92.7	47.1

** AT LEAST ONE ASSUMED RELATIVE HUMIDITY VALUE WAS USED IN THE INTERPOLATION.

STATION ALTITUDE 3969.0 FEET MSL
6 JULY 84   1300 HRS MST
ASCENSION NO. 255

WBN MANDATORY LEVELS
768CC?866
WHITE SANDS

SEODETIC COORDINATES
32.40843 LAT DEG
106.37033 LON DEG

GEOPOTENTIAL ALTITUDE DECAMETERS	WIND DATA				DEW PT DEP DEG C	TEMPERATURE AIR DEG C	PRESSURE MILLIBARS
	DIRECTION DEG (TN)	SPEED MPS	N-S MPS	E-W MPS			
2875.	97.	24.	1.	-24.	99	-41.7	1.500+1
2662.	66.	25.	-2.	-24.	99	-45.1	2.000+1
2566.	66.	17.	-2.	-18.	99	-52.0	2.500+1
2419.	97.	11.	-1.	-11.	99	-55.4	3.000+1
2283.	107.	13.	-4.	-12.	99	-55.4	4.000+1
2142.	96.	13.	-2.	-13.	99	-56.7	5.000+1
2073.	96.	13.	-2.	-13.	09	-61.8	6.000+1
1993.	94.	17.	-1.	-17.	96	-54.7	7.000+1
1802.	66.	6.	-9.	-4.	99	-56.1	8.000+1
1687.	117.	9.	-0.	-7.	99	-71.2	1.000+2
1534.	96.	9.	-7.	-4.	09	-69.2	1.250+2
1444.	27.	9.	-4.	-1.	99	-56.0	1.500+2
1369.	347.	9.	9.	0.	09	-50.5	1.750+2
1244.	356.	6.	6.	-2.	09	-53.9	2.000+2
1097.	24.	7.	7.	-3.	15	-42.9	2.500+2
974.	148.	6.	-4.	-4.	17	-35.3	3.000+2
851.	156.	8.	-7.	-4.	17	-27.5	3.500+2
762.	161.	101.	10.	-1.	19	-17.0	4.000+2
673.	144.	7.	-6.	-4.	22	-10.5	4.500+2
571.	132.	5.	-6.	-5.	22	-7.1	5.000+2
515.	101.	9.	-7.	-4.	22	-1.8	5.500+2
446.	84.	6.	-1.	-4.	99	2.5	6.000+2
359.	123.	4.	-5.	-2.	11	5.1	7.000+2
291.	204.	6.	5.	2.	13	15.1	7.500+2
205.	194.	5.	6.	1.	16	20.2	8.000+2
163.	191.	5.	6.	-1.		22.7	8.500+2